Journal of Food Engineering 404 (2026) 112769

Contents lists available at ScienceDirect

Journal of Food Engineering

journal homepage: www.elsevier.com/locate/jfoodeng

Performance of PBS materials with degradable additives for food packaging

Cristina Moliner [a], Emanuela Drago [a,*], Alberto Lagazzo [a], Samantha Caputo [b], Margherita Pettinato [a], Elisabetta Finocchio [a], Patrizia Perego [a], Jelena Barbir [c], Elisabetta Arato [a,b]

[a] Department of Civil, Chemical and Environmental Engineering (DICCA), University of Genoa, Via Opera Pia 15, 16145, Genova, Italy
[b] Tecnologie Innovative per Il Controllo Ambientale e Lo Sviluppo Sostenibile Scrl (TICASS), Via Domenico Fiasella, 3/16, 16121, Genova, Italy
[c] FTZ-NK, Faculty of Life Sciences, Hamburg University of Applied Sciences, Ulmenliet 20, 21033, Hamburg, Germany

ARTICLE INFO

Keywords:
Food contact material
Migration test
Water uptake
Differential scanning calorimetry
Fourier transform infrared spectroscopy
Young's modulus
Scanning electron microscopy

ABSTRACT

This study evaluates the physicochemical, mechanical, thermal and morphological properties of PolyButylene Succinate (PBS)-based bioplastics reinforced with degradable additives for food packaging applications. Water uptake tests revealed increased hydrolytic degradation at higher temperatures, particularly in ethanol-based simulants (from D = 0.0422•10^8 cm^2/s at 4 °C to 3.3491•10^8 cm^2/s at 40 °C). Migration tests confirmed compliance with EU regulations in acetic acid but some limitations to its suitability for alcoholic solutions, due to the overcome of overall migration limits (10 mg/dm^2). Specific migration of metal species was below EU limits, especially Co (<0.005 mg/kg) and Cr (0.0004 mg/kg), but is worthy of attention for packaging surface design. Mechanical analysis showed changes in the properties of the specimens after treatment, such as a slight increase in brittleness after exposure to acetic acid, coupled with a small increase in Young's modulus from 1.46 GPa to 1.65 GP, and a significant reduction in strain at break of about 37 % in ethanol-treated specimens, as also evidenced by the surface degradation shown by SEM analysis. FTIR-ATR analysis after treatments in ethanol and acetic acid solutions evidenced only few changes in main polymer chain, due to some limited hydrolysis of the PBS chain. Apparently, additives are mainly affected by the soaking in solutions, namely in the case of ethanol 50 % treatment at low temperature. DSC confirmed additive interactions and structural modifications. The results suggest that PBS-based materials are viable for food products with a pH < 4.5 under refrigerated conditions but require formulation adjustments for broader applicability.

1. Introduction

The growing demand for sustainable packaging is driven by environmental concerns and increased consumer awareness (Moeini et al., 2022; Hussain et al., 2024). In response, the European Commission-funded project BIO-PLASTICS EUROPE (https://bioplasticseurope.eu/) aims to develop eco-friendly alternatives to conventional plastics. The project initially focused on enhancing polylactic acid (PLA) and polybutylene succinate (PBS)-based materials by incorporating organic and inorganic fibers to improve their mechanical, thermal, and chemical properties. Some of these biopolymers were later re-engineered to address performance limitations (Cabrini et al., 2023; Agustin-Salazar et al., 2022; Arrieta et al., 2022).

PBS, synthesized from renewable sources like succinic acid and 1,4-butanediol, is a biodegradable and bio-based polymer with good mechanical strength, biodegradability, and compatibility with conventional processing methods (Platnieks et al., 2021; Shen, 2023). PBS can be produced from different feedstocks, some of which could compete with food production. However, recent production of PBS has been focused mainly on second or third generation feedstock in order to improve material's sustainability. Sustainability of innovative bio-based materials is crucial for its implementation to the market, since it deals with all three pillars o0f sustainability: environmental, economic and social. The environmental benefits of PBS are highlighted by its ability to decompose into water, carbon dioxide and biomass under composting conditions. This feature significantly reduces the impact of plastic waste on ecosystems, addressing a critical challenge posed by conventional petroleum-based plastics (Barletta et al., 2025). Moreover, the versatility of PBS allows for the development of different packaging formats, including films, bags and containers, meeting different market needs

* Corresponding author.
E-mail address: emanuela.drago@unige.it (E. Drago).

https://doi.org/10.1016/j.jfoodeng.2025.112769
Received 24 February 2025; Received in revised form 4 July 2025; Accepted 5 August 2025
Available online 6 August 2025

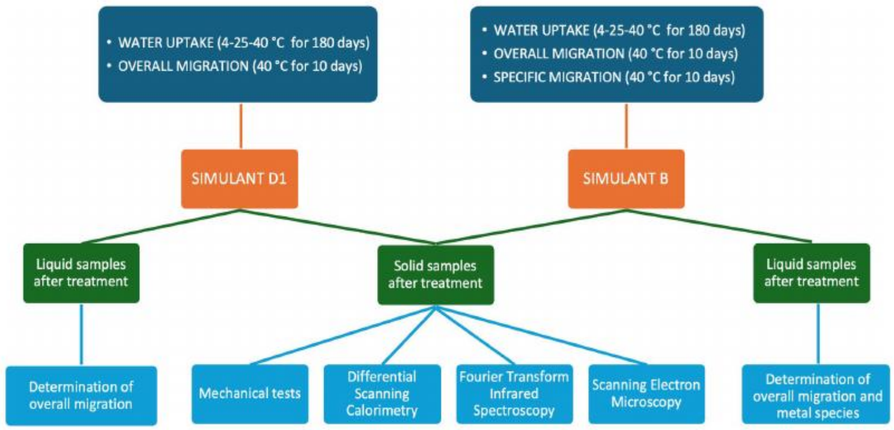

Fig. 1. Summary of experimental plan.

(Cheng et al., 2024).

Regarding the economic aspect, research and development activities continuously improve the performance and cost-effectiveness of PBS-based packaging. Innovations in polymer blending, additive incorporation and processing technologies are expanding their applicability and market competitiveness (Barletta et al., 2022). In order to successfully implement an innovative material to the market, it is essential to consider social acceptance of it and transition from fossil-based to bio-based materials. In order to achieve this social movement, it is crucial to achieve desirable technical, economic and environmental advancements in production of the materials. These advancements are key to driving the adoption of PBS as a mainstream material in the packaging industry, where PLA still leads the field with an annual production of 140,000 tonnes (Lagazzo et al., 2025). When designing new packaging materials, it is essential to fulfill specific requirements regarding mechanical, chemical and thermal performance, barrier properties and potential migration of compounds from the biopolymer to the food (European Commission, 2011). PBS is flexible, tough, and resistant to mechanical stress, meaning that PBS mechanical properties are stable across a wide temperature range, making it more versatile for long-term use. PBS is ideal for applications that require high flexibility, durability, and thermal stability, while in comparison PLA shows very good rigidity and clarity and it performs better in low-temperature environments because of its limited heat resistance. PBS is considered as one of the most reliable biodegradable plastics (bio-based) used in food packaging (Pedroni et al., 2023). Its slower crystallization rate also complicates the manufacturing process, resulting in longer production times and higher costs, which limits its large-scale adoption compared to conventional plastics such as polyethylene (PE) or polypropylene (PP). Inorganic fillers can significantly improve the mechanical and thermal properties of biopolymers (Rajgond et al., 2024). These fillers, such as talc, mica, calcium carbonate and nanoclays, strengthen the polymer matrix, improving stiffness and thermal resistance (Fajdek-Bieda and Wróblewska, 2024). In this context, this study aims to evaluate the structural and functional performance of newly developed PBS-based biopolymers with inorganic fillers for use in single-use soft packaging. Specifically, it investigates how food contact affects these materials by examining structural changes and potential degradation in various food simulants.

2. Materials and methods

2.1. Materials description

A PBS-based polymer (85–90 wt%, PBE grade 003, Mn ~ 50,000–60,000 g/mol, Mw ~ 160,000–180,000 g/mol) with mineral fillers (talc <15 % by weight), processed initially by twin-screw extrusion (temperature profile: 140–155 °C) and subsequently by injection moulding (temperature profile: 155–165 °C) supplied by NaturePlast (NPL, France), was designed to be used as soft packaging (SP) in food containers, such as yoghurt pots. The bio-based plastics were formed into dumbbell-shaped test bars with dimensions of 74.5 mm in length and 2 mm in thickness. The samples were tested as part of the BIO-PLASTICS EUROPE project (Grant Agreement n. 860407). The samples were labelled as SP-X-T, where "X" denotes the simulant (3 % w/v acetic acid and 50 % v/v ethanol) (European Commission, 2011), and "T" denotes the applied temperature (4 °C or 40 °C), as defined by European regulation to simulate the conditions of the food contained by the SP material. To compare the performance of the material before and after food contact, reference material as such, labelled as SP-REF-25, were also tested. A summary of the experimental plan is provided in Fig. 1.

2.2. Water uptake measurements

Samples were immersed (in triplicate) during 180 days in two different simulants to simulate various foods, including cloudy beverages containing fruit pulp, canned meat in aqueous medium and dairy products such as yoghurt, fermented milk, sour cream cheese and cheeses preserved in aqueous medium (e.g. feta, mozzarella). Immersions were conducted at two testing temperatures (4 °C and 40 °C). Solutions were prepared using a citrate-phosphate buffer provided by Sigma Aldrich. In addition, a further SP sample was tested using deionized water at 25 °C as a reference. In total, 15 specimens were tested, corresponding to 3 repetitions for deionized wáter at room temperature, 3 repetitions for simulant B at 4 °C, 3 repetitions for simulant B at 40 °C, 3 repetitions for simulant D1 at 4 °C and 3 repetitions for simulant D1 at 40 °C.

The water uptake tests were performed according to BS EN ISO 62:2008. The experimental and analytical procedures are described in detail elsewhere (Moliner et al., 2020). Briefly, the samples were removed from the solutions, dried superficially and weighed using a Sartorius analytical balance (w_t, accuracy 0.1 mg), and then re-immersed in the corresponding solutions at specific sampling times,

Table 1
Overall migration tests conditions, correction coefficients, and limits reported by the EU Reg. October 2011 (European Commission, 2011), and adopted in this study.

Simulant	Test conditions	Type of intended use	Limit EU Reg. 10/2011, Art. 12 (mg/dm²)
B = Acetic Acid 3 % w/v	10 days at 40 °C (single use)	To simulate 30 days at 4–5 °C (generally the expiration date of yoghurt is fixed 30 days after packaging)	10
D1 = EtOH 50 % v/v			10

depending on the trend of water uptake. The average content of absorbed water, M_t, was calculated by weigh difference (1) from the initial weight (w_0).

$$M_t = \frac{w_t - w_0}{w_0} \cdot 100 \tag{1}$$

An initial characterization of the properties was performed to establish the basic conditions of the samples. Water uptake measurements were carried out until stabilization. The saturation weight, M_s, was calculated as the value of M_t at the equilibrium (asymptotic line). Diffusivity was studied using the Fickian model via the Stefan's approximation, as described in detail elsewhere (Moliner et al., 2020). At the end of the test period, migration tests (global and specific) and mechanical, thermal, chemical and morphological analyses were performed.

2.3. Migration tests

2.3.1. Overall migration tests

The samples were subjected to overall migration tests according to ISO 1186 (European Standards, 2002). For each type of material supplied, the most severe test conditions were selected in terms of food simulant, exposure temperature and simulant contact time. These parameters depend on the intended end-use application, reported in Section 2.2, according to European Regulations (2020)/1245 (European Commission, 2020), amending and correcting EU Regulation October 2011 (European Commission, 2011) on plastic materials and articles intended to come into contact with foodstuff. Table 1 shows the details of the conditions adopted for the overall migration tests. All the experiments were performed in triplicate under controlled temperature conditions. According to Regulation, the volume of the food simulant was assessed to keep the S/V ratio between the surface area of the sample exposed to the simulant (cm^2) and the volume of the simulant (cm^3) constant and equal to 0.6. The surface area of each sample was measured using ImageJ software (NIH, Bethesda, MD, USA). The overall migration was evaluated gravimetrically, after complete drying of the simulant containing the migrated material at 105 °C until a constant weight was reached.

All the experiments were performed in triplicates and the results were expressed through descriptive statistical analyses using Statistica v 12.0 software (StatSoft, Tulsa, OK, USA). Descriptive statistic was adopted for migration tests to better contextualize results in terms of compliance with the well-defined limits imposed by Regulations, thus emphasizing deviations related to potential experimental errors and variability among samples.

2.3.2. Specific migration tests for heavy metals detection

The specific migration tests (ISO 13130) (European Standards, 2004), for the detection of metal species (Cobalt, Chromium, Iron, Manganese, Nickel, Copper, and Zinc), according to the procedures established by EU Regulation 2020/1245, amending and correcting EU Regulation 10/2011, were performed at the temperature and time conditions indicated in Table 1. The simulant reproducing the most severe conditions (acetic acid 3 % w/v) was adopted. After the migration tests, the liquid simulants were filtered (0.45 μm) and analyzed by an atomic absorption spectrometer (Varian AA240Z, Markham, ON, Canada) equipped with a graphite furnace (GTA 120280) for the quantification of the metal species. All the experiments were performed three times, and the results were expressed through descriptive statistical analyses using the Statistica v 12.0 software (StatSoft, Tulsa, OK, USA). Descriptive statistic was adopted only for migration tests to better contextualize results in terms of compliance with the well-defined limits imposed by Regulations, thus emphasizing deviations related to potential experimental errors and variability among samples.

2.4. Mechanical Characterisation

Static tests to obtain the mechanical properties of the samples were obtained using a Zwick/Roell Z50 electro-mechanical universal testing machine, equipped with a makroXtens II modular arm strain gauge and 50 KN load cell. The data were collected and analyzed using testXpert III software. The test was performed before (untreated specimen SP-NT) and after the two migration tests (specimens SP-B-40 and SP-D1-40) and after the water uptake tests (specimens SP-REF-25, SP-D1-4, SP-B-4) to investigate possible structural changes. Tensile tests were performed according to DIN EN ISO 527-1 on dog-bone samples at room temperature.

All the tests were performed at a speed of 1 mm/min, for the determination of the tensile elastic modulus, and at a speed of 50 mm/min until break. The mechanical results obtained from these tests were Young's modulus at tensile stress, ultimate tensile strength UTS, i.e. the maximum stress recorded during the test, strain at UTS, stress at breaking and strain at breaking.

2.5. Differential scanning calorimetry (DSC)

Thermal properties were analyzed using differential scanning calorimetry (DSC) in a Netzsch Differential scanning Calorimeter 300 Caliris. Data were collected and processed using Proteus 9.2 software.

Each sample was cut into one or two blocks for a total of about 15 mg, placed in an aluminum crucible and then sealed with a top in which a small hole was drilled to allow the gas produced during testing to escape. All the analyses were carried out between −10 °C and 220 °C at a rate of 20 °C/min in nitrogen.

2.6. Fourier Transform Infrared spectroscopy (FTIR-ATR)

Chemical characterization by analysing FTIR-ATR spectra was performed using a FT Nexus Thermonicolet instrument equipped with an ATR accessory (diamond window), 100 scans, 4 cm^{-1} resolution, DTGS detector, background air. Spectra were collected in the range 4000-400 cm^{-1} (mid-IR region).

Each analysis was repeated in different samples or in at least two different points of the same sample. The discussion reported in the following paragraphs is based on the comparison between the spectra of pristine material and the spectra collected after the different treatments in the solutions shown in Table 1.

2.7. Scanning electron Microscopy (SEM)

Morphological analysis was performed with a Hitachi S-2500 scanning electron microscope (SEM) in secondary electrons. The analysis was conducted before (SP-NT) and after the two migration tests (samples SP-B-40 and SP-D1-40) and after the water uptake tests (samples SP-REF-25, SP-D1-4, SP-B-4) to investigate any morphological changes. A portion of approximately 5 mm was obtained from the samples used for the tensile tests. The samples were observed, after gold coating, on the outer surface at 100x and 500× magnification.

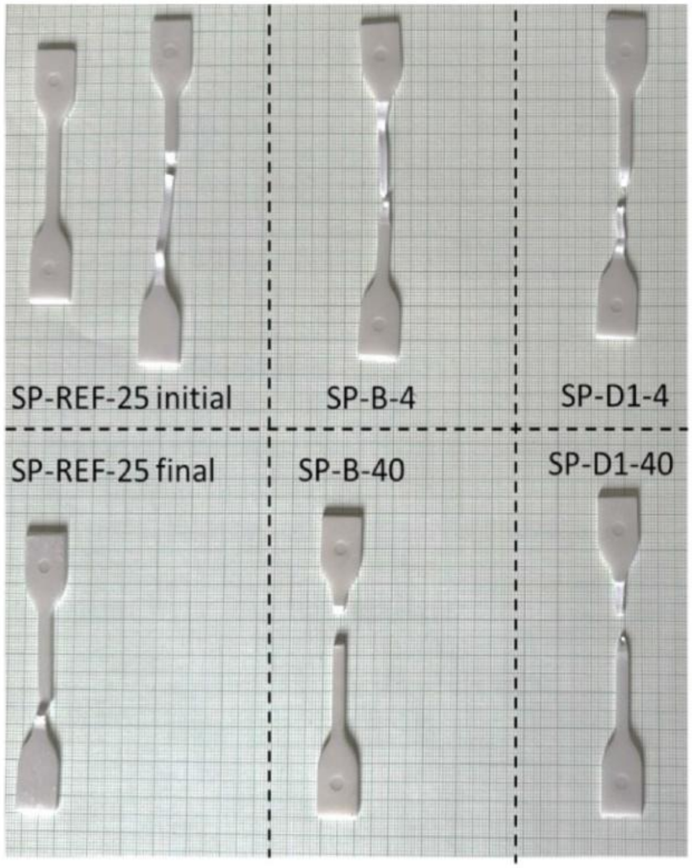

Fig. 2. Physical appearance of tested samples before and after treatment.

Table 2
Saturation weight (M_s, %) with experimental deviation and diffusion coefficients (D, cm^2/s) at all tested conditions. For comparison, the reference material (SP-REF-25) presented a $M_s = 0.6415$ % and a D = 2.87.

Food simulant	4 °C		40 °C	
	Ms [%]	D•10[8]	Ms [%]	D•10[8]
B	0.9504 ± 0.0016	0.1963	>6.28	–
D1	2.3360 ± 0.0476	0.0422	3.5358 ± 0.0603	3.3491

3. Results and discussion

3.1. Absorption of water by PBS-based biopolymers

Water absorption tests were conducted in deionized water and two food simulants (B and D1) at 4 °C and 40 °C to assess the hydrolytic behavior of PBS-based bioplastics under refrigerated and accelerated mass transfer conditions, respectively, that simulate real-life usage, such as soft packaging for moist products like yoghurt. Fig. 2 presents the visual appearance of the biopolymer specimens before and after exposure, highlighting noticeable changes, particularly at higher temperatures. The water uptake behavior was quantitatively assessed through the calculation of saturation water content (M_s, %) and diffusion coefficients (D, cm^2/s), which are summarized in Table 2. These parameters provide insights into the extent and rate of water penetration into the polymer matrix, which are critical for understanding long-term material performance.

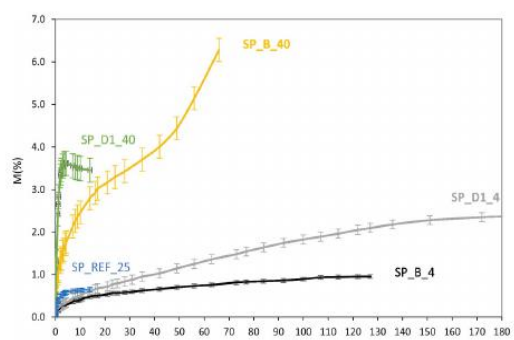

Fig. 3. Water uptake profiles.

Table 3
Descriptive statistics on overall migrations results obtained from tests on SP. Simulant B: acetic acid 3 % w/v; simulant D1: EtOH 50 % v/v.

M [mg/dm^2]	SD [mg/dm^2]	I.C. −95 % [mg/dm^2]	I.C. +95 % [mg/dm^2]	Min [mg/dm^2]	Max [mg/dm^2]	Std. error [mg/dm^2]	Limit EU Reg. [mg/dm^2]
Simulant B – 40 °C, 10 days							
4.91	2.53	0.00	11.20	2.95	7.77	1.46	10
Simulant D1 – 40 °C, 10 days							
28.48	5.12	15.77	41.19	22.67	32.32	2.95	10

Note: Results are reported as mean value of migration (M) and its standard deviation (SD). Results obtained by the descriptive statistical analysis are expressed as Interval of Confidence (I.C.), minimum and maximum values (Min, Max) and standard error (Std. error).

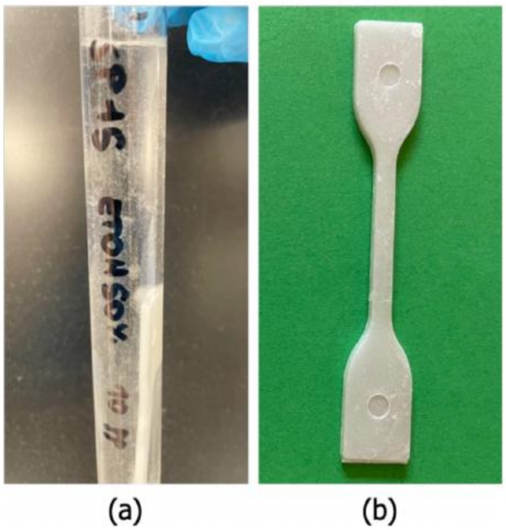

Fig. 4. Release liquid (a) and specimen (b) appearance of SP samples after migration test conducted at 40 °C for 10 days in simulant D1.

As expected, water uptake increased with increasing temperature, as the diffusivity coefficient, D, did. Furthermore, the samples immersed in alcohol solution (simulant D1) had higher values of saturation weight, which corresponds to a low water diffusion rate in the bio-based polymer, as was the case in the first material formulation (Finocchio et al., 2023). In contrast, samples in simulant B at 40 °C absorbed water rapidly without reaching equilibrium (Fig. 3), suggesting possible structural degradation in acidic conditions at elevated temperatures. Compared to the reference material (SP-REF-25), the samples demonstrated higher water uptake, particularly in acidic environment, but diffusion behavior varied depending on temperature and medium. These results highlight that while the material is suitable for cool and dry storage, its performance may be compromised in warm, acidic, or alcohol-rich environments.

3.2. Results from the overall migration

Table 3 reports the results of the overall migrations tests, showing the mean values of the overall migration (M) for each round, expressed, as for the Regulations, in mg of migrated substance per dm^2 of sample area, and the respective standard deviations (SD), confidence intervals (I.C.), minimum and maximum values (Min, Max), and standard errors, respectively.

Samples exposed under accelerated mass transfer conditions (40 °C for 10 days) to acetic acid 3 % w/v were found to comply with the limit of the EU Regulation 2020/1245 (European Commission, 2020), so the bio-based material could be suitable for contact with foodstuff with a pH < 4.5 stored under the desired real-word conditions, i.e. at refrigerated temperature for 30 days. The overall migration values obtained in simulant D1 were above the EU Regulation limit. The significant mass transfer observed with this food simulant was confirmed by the suspension present in the liquid after release and by the surface of the specimens, which was non-homogeneous in colour after testing (Fig. 4). Migration from the samples placed in contact with ethanol 50 % v/v can be partially traced back to the hydrolysis of the material, due to water molecules that can cause the mobility of the chains and increase the free volume, inducing hydrolytic degradation resulting in the breakage of the PLA chains (Limsukon et al., 2023). Furthermore, ethanol plasticises the PLA matrix, improving the mobility of the chains and the rate of degradation of the polymer (Iñiguez-Franco et al., 2017). Xu et al. (2023) reported that interactions between PLA and organic solvents can cause swelling or plasticisation of the polymer matrix, compromising its performance. In particular, in contact with ethanol and water solutions, the absorption and diffusion of the alcohol through the polymer generates swelling and rearrangement of the polymer chains. In addition, the high affinity of some additives in the PLA formulation toward ethanol and lipophilic environments may further contribute to migration in food simulants, as confirmed in Section 3.6 and supported by a recent study highlighting specific interactions of additives with polar solvents (Dragan et al., 2024). Taken together, these results indicate that

Table 4
Descriptive statistics about results of specific migration of metal species into the tested simulants.

Metal	MS [mg/kg]	SD [mg/kg]	I.C. −95 % [mg/kg]	I.C. +95 % [mg/kg]	Min [mg/kg]	Max [mg/kg]	Std. error [mg/kg]	EU Reg. Limit [mg/kg]
Co	<0.005	–	–	–	–	–	–	0.05
Cr	0.0004	0.0004	0.0001	0.0007	0.0001	0.0010	0.0001	0.01
Cu	0.0538	0.0359	0.0263	0.0814	0.0266	0.1047	0.0120	5
Fe	0.0817	0.0438	0.0480	0.1154	0.0044	0.1341	0.0146	48
Mn	0.0012	0.0004	0.0009	0.0015	0.0007	0.0019	0.0001	0.6
Ni	0.0011	0.0003	0.0009	0.0014	0.0004	0.0015	0.0001	0.02
Zn	0.1052	0.0291	0.0783	0.1321	0.0614	0.1350	0.0110	5

Note: Results are reported as mean concentration of the metal and standard deviation (SD). Results obtained by the descriptive statistical analysis are expressed as Interval of Confidence (I.C.), minimum and maximum values (Min, Max) and standard error (Std. error). The specific migration values (MS) must then be corrected on the basis of the final surface area of the foodstuff to be packaged $= \frac{MS\ sample \cdot Area\ finished\ product}{0.169 \pm 0.002\ dm^2}$.

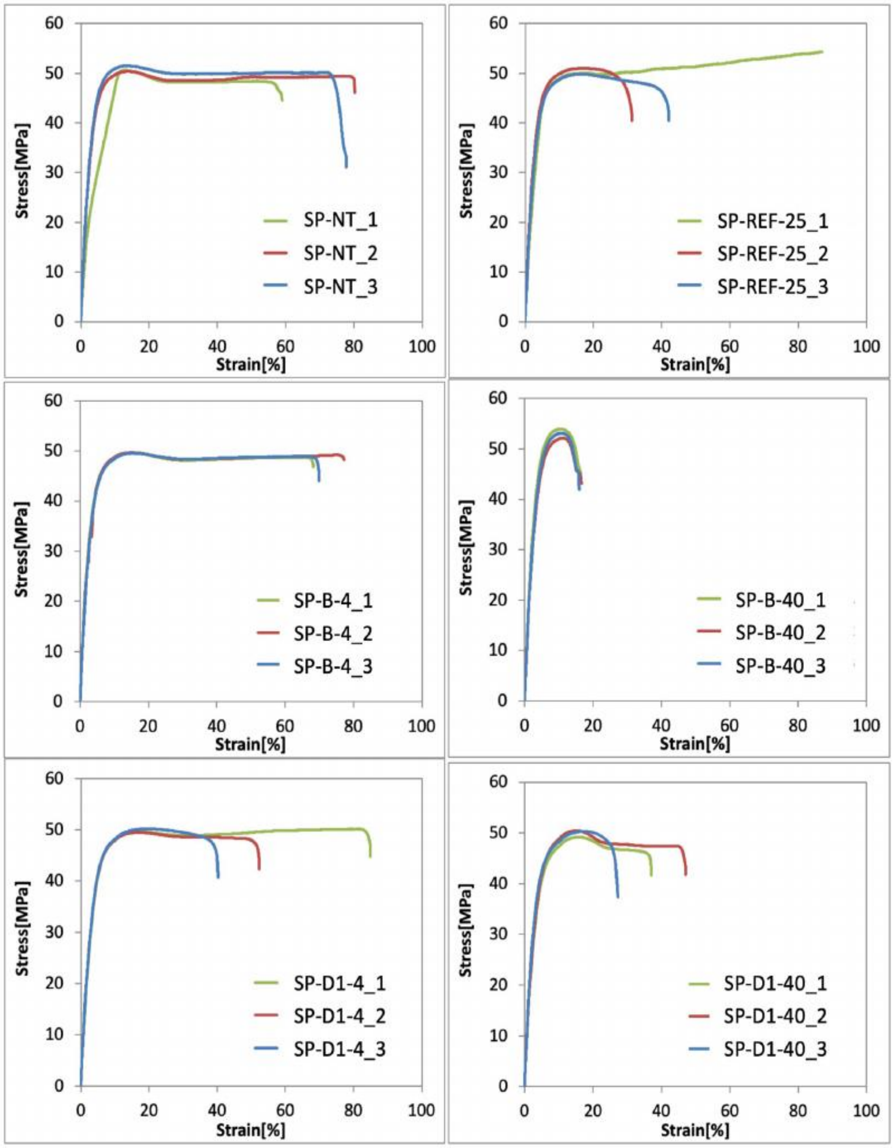

Fig. 5. Stress vs. strain diagrams of tensile test on SP samples after the different treatments.

the material does not meet the overall migration limits imposed by EU Regulation 2020/1245 (European Commission, 2020) and therefore is not suitable for contact with food products with high alcohol content (>20 %), oil-in-water emulsions, or fatty foods stored under refrigerated conditions for prolonged periods (≥30 days). This is consistent with recent literature that emphasizes the need for specific evaluations for PLA-based packaging materials, especially in the presence of complex food matrices (Xu et al., 2023; Khajavi et al., 2022).

3.3. Results from the specific migration

Table 4 shows the specific migration (MS) values of SP samples after tests conducted for 10 days at 40 °C in 3 % w/v acetic acid. Unlike the overall migration, which is expressed as mg of substance released per dm^2 of surface area of packaging material sample, the specific migration is expressed as mg of substance released per kg of foodstuff/food simulant based on the actual surface area/volume ratio for the intended or foreseeable use, according to Article 17 of Regulation EU10 of 2011 (L12/12). Notably, the mean concentration of all metals was recorded below the limits of the EU Regulation. This result was also demonstrated

Table 5
Young modulus (E_t), ultimate tensile stress (σ_M) and strain (ε_M), and strain at break (ε_b) of SP benchmark samples and after the different treatments.

	Young's Modulus	Ultimate Strength	Strain at UTS	Strain at Break
	E_t [GPa]	σ_M [MPa]	ε_M [%]	ε_b [%]
SP-NT	1.46 ± 0.30	50.81 ± 0.58	13.32 ± 0.34	72.31 ± 11.24
SP-D1-40	1.49 ± 0.06	49.97 ± 0.70	16.03 ± 1.00	37.13 ± 9.96
SP-B-40	1.66 ± 0.05	53.08 ± 0.90	10.86 ± 0.05	16.28 ± 0.35
SP-REF-25	1.55 ± 0.13	51.97 ± 2.79	43.41 ± 46.72	60.02 ± 40.70
SP-D1-4	1.36 ± 0.03	49.95 ± 0.39	39.09 ± 36.38	59.17 ± 23.13
SP-B-4	1.56 ± 0.06	49.63 ± 0.07	15.21 ± 0.52	71.76 ± 4.76

by the maximum values (Max) and confidence intervals (I.C.), derived from the descriptive statistical analysis.

In a study conducted by (Peng et al., 2023a) the leaching of metals from PLA in seawater was analyzed. Their study confirmed that at 40 °C metal leaching is not negligible as at 25 °C, due to temperature effect that promotes the diffusion of the additive metals in the polymer matrix and their migration.

In the samples analyzed, Zn is the most migrated metal. The presence of such metal species is commonly found in plastics, due to Zn-based chemicals, which are widely employed in a variety of processes manufacturing plastics (Peng et al., 2023b). Despite the high variability among the samples, the specific metal migration values of all the replicates were found to be below the limit set by legislation.

Nevertheless, the quantitative specific migration depends on the final surface area of the foodstuff to be packaged.

3.4. Results from the mechanical characterisation

The stress-strain behavior of the PBS-based specimens reflects that of a typical soft polymer, showing a marked plastic deformation after an initial elastic region, with a failure occurring at approximately 70 % strain (Fig. 5). Notable variability was observed in some of the treated samples, particularly those exposed to simulant D1 at 40 °C, suggesting structural heterogeneity or degradation induced by ethanol exposure.

Mechanical performance after immersion showed clear differences depending on the type of simulant and treatment temperature. Exposure to 3 % acetic acid (simulant B) at 40 °C resulted in the most significant degradation: a dramatic reduction in strain at break from 70 % to approximately 15 %, indicating strong embrittlement. This was accompanied by a slight increase in Young's modulus from a value of 1.46 GPa–1.65 GP (Table 5), implying reduced molecular mobility. In contrast, immersion in 50 % ethanol (simulant D1) at 40 °C caused a moderate decline in strain at break to 37 %, with minimal changes in stiffness. This suggests that ethanol may plasticize or alter the polymer surface without significantly affecting bulk stiffness. Interestingly, exposure to either simulants at 4 °C did not significantly alter the mechanical response compared to the reference sample (SP-NT), confirming that temperature plays a critical role in accelerating degradation or structural changes. Across all treatments, the ultimate tensile strength (UTS) remained largely unaffected, with values consistently around 50 MPa. This indicates that while stiffness may vary, the material retains its load-bearing capacity up to the point of failure.

These findings highlight that mechanical durability of PBS-based bioplastics is highly sensitive to environmental conditions, particularly to acidic environments at elevated temperatures. Such insights are essential when evaluating their suitability for specific packaging applications where exposure to acidic or alcoholic food products is expected.

3.5. Results from the morphological characterization

The untreated SP specimens show a smooth surface shown in Fig. 6. In the strained part near the fracture, transverse linear microfractures about 10 μm apart are evident (Fig. 6), indicating localized stress concentration during mechanical testing. Exposure to different food simulants causes distinct morphological alterations on the specimen surfaces,

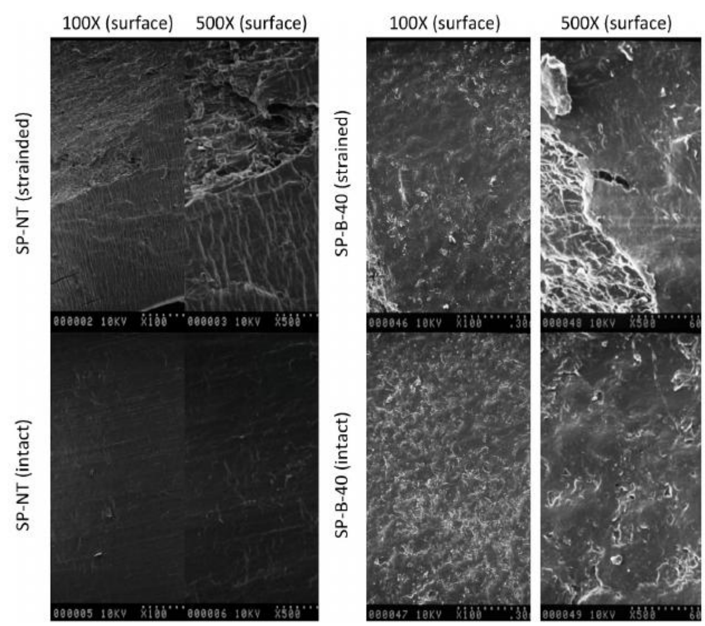

Fig. 6. SEM images at ×100 and ×500 of SP samples not treated and SP-B (Acetic Acid 3 %, 40 °C).

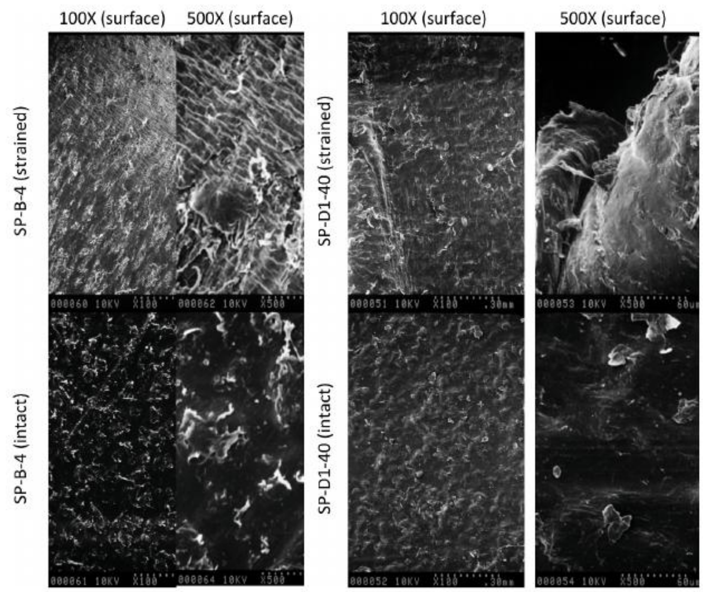

Fig. 7. SEM images at ×100 and ×500 of SP-B (Acetic Acid 3 %, 4 °C) and SP-D1 (EtOH 50 %, 40 °C) samples.

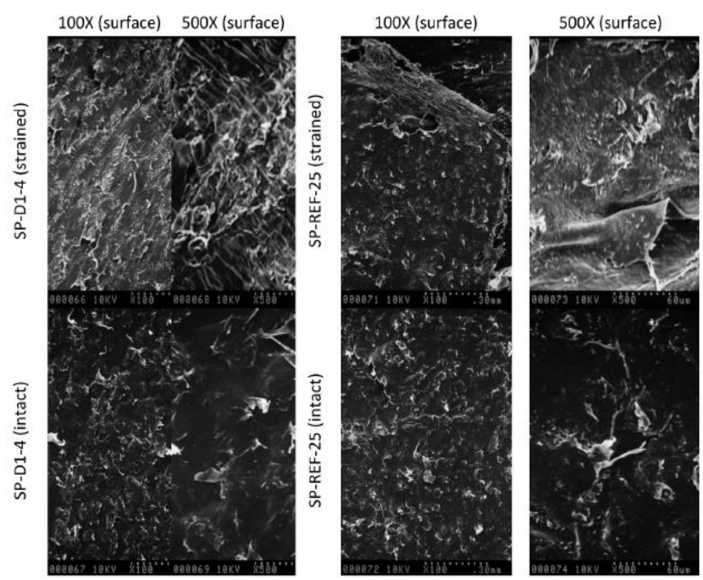

Fig. 8. SEM images at ×100 and ×500 of SP-D1 (EtOH 50 %, 4 °C) and SP (Deionized water, 25 °C) samples.

as shown in Fig. 7. Interestingly, the SP-B-40 samples (treated in 3 % acetic acid at 40 °C) display relatively smooth surfaces, similar to the untreated ones. However, these samples develop irregularly shaped microcracks of varying size. Although surface damage appears limited, this contradicts the significant embrittlement observed in mechanical testing. This apparent discrepancy may be reconciled by considering the formation of subsurface microcracks that penetrate deeper into the polymer matrix, weakening the material internally without drastically affecting surface appearance.

In other SP samples, the surface roughness increases due to the partial exposure of irregularly shaped bulk microparticles, ranging in size from 10 μm to 50 μm. This roughness probably results from the removal of the outer layer caused by treatment. In particular, SP-D1-4 samples show the most pronounced effects, with sharp and irregular

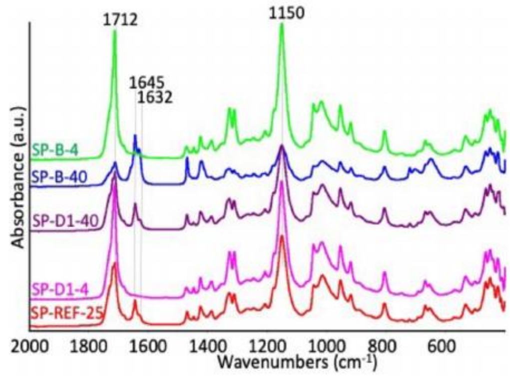

Fig. 9. ATR IR spectra of samples SP (benchmark spectrum is reported for comparison).

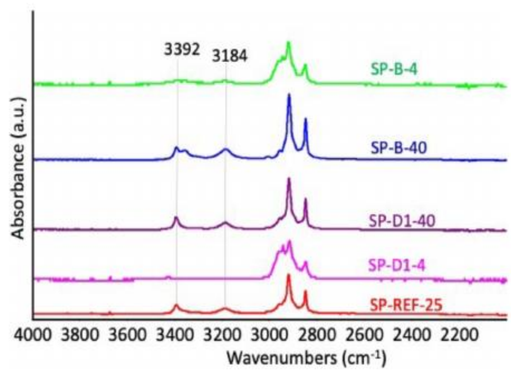

Fig. 10. ATR IR spectra of samples SP (benchmark spectrum is reported for comparison). High frequency region.

flakes emerging from the surface and partially peeling off (Fig. 8). This peeling indicates delamination or localized swelling and shrinkage cycles, which may result from ethanol's plasticizing or solvent action on the polymer surface. Overall, the surface analysis confirms that environmental exposure leads to structural and morphological changes, although the extent and visibility of degradation depend strongly on both simulant type and temperature. These observations complement the mechanical results, highlighting a complex degradation behavior involving both surface and subsurface mechanisms.

3.6. Results from the FTIR-ATR characterisation

The spectrum of the reference SP sample shows a complex main band centred at 1712 cm^{-1} and a weaker band at 1645 cm^{-1} with a shoulder at 1632 cm^{-1} (Fig. 9). The former component is due to C=O stretching of the ester group in the main PBS chain and its complexity has been explained by the presence of amorphous and crystalline fractions in the material, with the maxima at 1712 cm^{-1} corresponding to carbonyl stretching of the crystalline fraction (Yao et al., 2017; de Matos Costa et al., 2020). The latter component is not typical of pure PBS and it could be due to C=C stretching modes in functional groups other than the ester, in agreement with the presence of additives in the formulation of the material. The band at 1150 cm^{-1} is assigned to the –C-O-C- stretching mode of ester bonding (Phua et al., 2011, 2013). In the high-frequency region of the spectrum (Fig. 10), in addition to the bands in the 3000-2800 cm^{-1} range due to the CH stretching modes, two weak absorption are detectable at 3392 and 3184 cm^{-1}, which are not directly related to the structure of PBS but are consistent with the presence of NH/NH_2 groups (amines and/or amides) whose corresponding strain modes may contribute to the complex signal near 1645-1630 cm^{-1}.

After treatment in ethanol 50 % v/v at 40 °C (SP-D1-40), the IR spectra of the different specimens showed marked variability in the relative intensities of the bands around 1645 cm^{-1} and the bands in the high-frequency region, probably corresponding to the additives in the material formulation. In a second set of spectra corresponding to samples treated in ethanol at 4 °C (SP-D1-4), these bands disappear almost completely, while the bands due to the polymer matrix do not change significantly in intensity and position. These results agree with the overall migration data showing changes in the specimen and release of materials into the surrounding liquid phase. In addition, following the same treatment, a weak band appears in the high-frequency region of the spectrum at 3430 cm^{-1}, which can be assigned to stretching of the terminal hydroxyl groups of PBS, suggesting some hydrolysis of the polymer chain (de Matos Costa et al., 2020). Another weak and sharp component is detected at 3675 cm^{-1}, probably due to the exposed OH groups of the mineral filler. The changes detected by spectroscopy are consistent with the results of SEM analysis, which indicate that sample SP-D1-4 shows deep surface degradation phenomena.

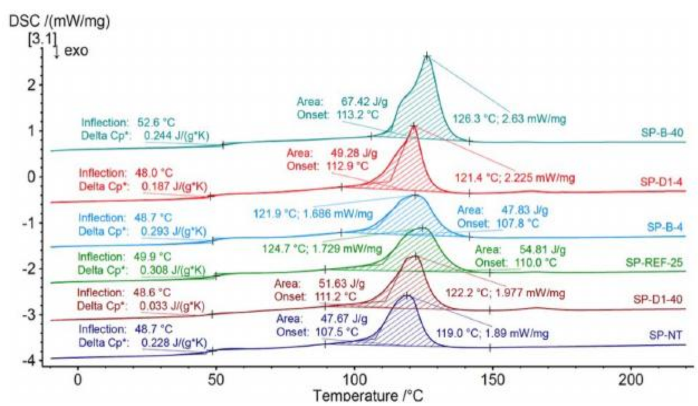

Fig. 11. DSC analysis of SP samples and after the different treatments. Endothermic (upward).

Table 6
Thermal parameters of the SP benchmark samples and after the different treatments.

Sample	Tg [°C]	Peak T [°C]	Onset T [°C]	Offset T [°C]	Peak DH [J/g]
SP-NT	48.7	119	107.5	127.1	+47.7
SP-REF-25	49.9	124.7	110.0	135.4	+54.8
SP-B-4	48.7	121.9	107.8	132.5	+47.8
SP-D1-4	48.0	121.4	112.9	127.1	+49.3
SP-B-40	52.6	126.3	113.2	133.3	+67.4
SP-D1-40	48.6	122.2	111.2	129.7	+51.6

The IR spectra of the samples after treatment in acetic acid 3 % w/v at 40 °C and 4 °C (SP-B-40 and SP-B-4) show some variability of the relative intensity of the main bands in the range 1715-1600 cm^{-1}. In particular, the intensity ratio between the band at 1712 cm^{-1} and the band at 1645 cm^{-1} changes without a clear trend, and this effect can be explained by the interaction of additives with acetic acid solutions. The high-frequency components between 3100 and 3500 cm^{-1} disappear almost completely in the spectra of sample treated at 4 °C, while another weak component at 3360 cm^{-1} becomes more prominent compared with the reference spectrum, probably due to the free hydroxyl groups of the inorganic filler and/or the end groups of the polymer chains. The spectrum of sample SP-B-40 actually shows weaker components than the original spectrum, and the bands assigned to additive species are still well defined, even increased in relative intensity. On the other hand, this is the sample whose surface appears smooth, although with some microfractures.

In this case, the ATR analysis, which is limited to the surface and subsurface layers, is not explanatory of the different mechanical properties detected, which could be mainly attributed to the bulk modification.

In summary, from spectroscopic studies, only few and limited changes in the spectra of the main polymer chain are evident after treatments in ethanol and acetic acid solutions only due to hydrolysis of the PBS chain. However, significant changes in spectral features, such as changes in relative intensities of the band, suggest that the additives are mainly affected by immersion in solutions, particularly in the case of treatment with ethanol 50 % at low temperature.

3.7. Results from the calorimetric characterisation

DSC analysis shows for all samples a higher endothermic peak, attributable to melting, between 119 °C for the NT samples and 126 °C for the SP-PBS-02-40°C-B samples, as can be seen in Fig. 11 and Table 6. This higher peak temperature value and the higher value of the subtended area ($\Delta H = +67.4$ J/g), corresponding to the enthalpy associated with melting, can be explained by a change in microstructure due to treatment in acetic acid at 40 °C. A higher heat of fusion, associated with a higher Tg, 52.6 °C compared to 48.7 °C in the NT sample, is related to the presence of stronger bonds between the organic chains (Kong and Hay, 2003). This fact, which is completely negligible or at least less evident in the samples subjected to the other treatments, with Tg values between 48.0 °C and 49.9 °C and enthalpy between 47.7 J/g and 54.8 J/g, is consistent with higher brittleness, as confirmed by mechanical tests. Although the change in the mechanical properties indicates that the degradation of the material is not limited to the surface but also involves the bulk of the sample, the presence of a shoulder peak at a temperature closer to that of the reference sample (Fig. 11) is an indication that not all the specimen is subjected to the degradation, but some of the material retains its original characteristics.

In summary, the results of this study highlight the complex interaction between the physicochemical, mechanical, thermal and morphological properties of PBS-based bioplastics when exposed to different food simulants. The combination of these techniques presents a comprehensive characterization of the material, illustrating its suitability for food products with a pH < 4.5 under refrigerated conditions, while emphasizing its limitations for oil-water emulsions or alcoholic solutions. These results provide valuable insights for the optimization of biopolymer formulations to improve their functional performance in targeted food packaging applications.

4. Conclusions

Poly(butylene succinate) (PBS), as a bio-based and biodegradable polymer, presents a promising eco-friendly alternative to conventional plastics, aligning with the objectives of sustainable packaging. The findings of this study reinforce the potential of PBS-based materials to replace traditional soft plastics, particularly in low-temperature food packaging applications. For instance, water uptake tests demonstrated that hydrolytic degradation of the material is more pronounced at higher temperatures and in alcohol-based simulants, consistent with trends observed in overall and specific migration tests. These tests confirmed that while the material complied with EU regulatory limits in acetic acid-based simulants, exposure to ethanol led to higher migration values, indicating incompatibility with lipophilic or high-alcohol foodstuffs. Mechanical tests further strengthened this finding, revealing that immersion in acetic acid at 40 °C induced brittleness, while ethanol treatments significantly reduced strain at break, suggesting structural degradation. In addition, morphological analysis provided complementary insights, with surface roughness and microfractures confirming the degradation mechanisms deduced from mechanical tests. Finally, spectroscopic analysis (FTIR-ATR) revealed changes in materials, particularly in the interactions of additives with simulants, while DSC analysis supported the presence of structural modifications, especially for samples exposed to acetic acid at elevated temperatures. In conclusion, PBS-based material are well-suited for food products with pH < 4.5 stored at refrigeration temperatures (4–5 °C) for up to 30 days. However, their use is not recommended for lipophilic foods or products containing more than 20 % ethanol, or for storage at room temperatures, due to significant structural and chemical degradation under these conditions.

CRediT authorship contribution statement

Cristina Moliner: Writing – review & editing, Writing – original draft, Validation, Methodology, Investigation, Formal analysis, Data curation. **Emanuela Drago:** Writing – review & editing, Writing – original draft, Validation, Methodology, Investigation, Formal analysis, Data curation. **Alberto Lagazzo:** Writing – original draft, Validation, Methodology, Investigation, Formal analysis, Data curation. **Samantha Caputo:** Validation, Project administration, Investigation, Formal analysis. **Margherita Pettinato:** Validation, Methodology, Investigation, Formal analysis, Data curation. **Elisabetta Finocchio:** Writing – original draft, Validation, Methodology, Investigation, Formal analysis, Data curation. **Patrizia Perego:** Supervision, Project administration. **Jelena Barbir:** Supervision, Project administration, Funding acquisition, Conceptualization. **Elisabetta Arato:** Validation, Project administration, Funding acquisition, Conceptualization.

Formatting of funding sources

This work has received funding from the European Union's Horizon 2020 Research and Innovation Programme through the research project BIO-PLASTICS EUROPE (Grant agreement No. 860407).

Declaration of competing interest

The authors declare that they have no known competing financial interests or personal relationships that could have appeared to influence the work reported in this paper.

Data availability

Data will be made available on request.

References

Agustin-Salazar, S., Ricciulli, M., Ambrogi, V., Cerruti, P., Scarinzi, G., 2022. Effect of thermal annealing and filler ball-milling on the properties of highly filled polylactic acid/pecan nutshell biocomposites. Int. J. Biol. Macromol. 200, 350–361. https://doi.org/10.1016/j.ijbiomac.2021.12.101.

Arrieta, M.P., Beltran, F., Abarca de las Muelas, S.S., Gaspar, G., Sanchez Hernandez, R., de la Orden, M.U., Martinez Urreaga, J., 2022. Development of tri-layer antioxidant packaging systems based on recycled PLA/sodium caseinate/recycled PLA reinforced with lignocellulosic nanoparticles extracted from yerba mate waste. Express Polym. Lett. 16, 881–900. https://doi.org/10.3144/expresspolymlett.2022.64.

Barletta, M., Aversa, C., Ayyoob, M., Gisario, A., Hamad, K., Mehrpouya, M., Vahabi, H., 2022. Poly(butylene succinate) (PBS): materials, processing, and industrial applications. Prog. Polym. Sci. 132, 101579. https://doi.org/10.1016/j.progpolymsci.2022.101579.

Barletta, M., Genovesi, A., Desole, M.P., Gisario, A., 2025. Melt processing of biodegradable poly(butylene succinate) (PBS)—A critical review. Clean Technol. Environ. Policy 27, 683–725. https://doi.org/10.1007/s10098-024-03005-8.

Cabrini, A., Ghalayani Esfahani, A., Petraconi, A., Lavorgna, M., De Nardo, L., Buonocore, G.G., Andrade, R.J.E., Cerruti, P., 2023. Ultrasonic spray deposition of PEGDE-crosslinked chitosan/graphene oxide coatings for enhancing gas barrier properties of polybutylene succinate films. Prog. Org. Coat. 183, 107760. https://doi.org/10.1016/j.porgcoat.2023.107760.

Cheng, J., Gao, R., Zhu, Y., Lin, Q., 2024. Applications of biodegradable materials in food packaging: a review. Alex. Eng. J. 91, 70–83. https://doi.org/10.1016/j.aej.2024.01.080.

de Matos Costa, A.R., Crocitti, A., Hecker de Carvalho, L., Carroccio, S.C., Cerruti, P., Santagata, G., 2020. Properties of biodegradable films based on poly(butylene succinate) (PBS) and poly(butylene Adipate-co-Terephthalate) (PBAT) blends. Polymers 12, 2317. https://doi.org/10.3390/polym12102317.

Dragan, V.K., Petrovics, N., Kirchkeszner, C., Tábi, T., Szabó, B.S., Eke, Z., 2024. The kinetics of swelling and migration: a case study of plasticized polylactic acid food contact plastics tested with ethanolic food simulants. Express Polym. Lett. 18 (4), 391–405. https://doi.org/10.3144/expresspolymlett.2024.29.

European Commission, 2020. Regulation (EU) 2020/1245 of 2 September 2020 which modified regulation n.10/2011 on plastic materials and articles intended to come into contact with food. Gazzetta ufficiale dell'Unione Europea 16, 1–17. https://eur-lex.europa.eu/eli/reg/2020/1245/oj/eng/. January 2025.

European Commission, 2011. Regulation (EU) no. 10/2011 of 14 January 2011 on plastic materials and articles intended to come into contact with food. https://eur-lex.europa.eu/eli/reg/2011/10/oj/eng/. January 2025.

European Standards, 2004. Materials and Articles in Contact with Foodstuffs — Plastics Substances Subject to limitation— Part 2: Determination of Terephthalic Acid in Food Simulants (ISO-13130-2:2004). British standards BS EN, pp. 13130–1:2004 3.

European Standards, 2002. Materials and Articles in Contact with Foodstuffs - Plastics - Part 1: Guide to the Selection of Conditions and Test Methods for Overall Migration. British standards BS EN, 1186-1:2002 49.

Fajdek-Bieda, A., Wróblewska, A., 2024. The use of natural minerals as reinforcements in mineral-reinforced polymers: a review of current developments and prospects. Polymers 16, 2505. https://doi.org/10.3390/polym16172505.

Finocchio, E., Moliner, C., Lagazzo, A., Caputo, S., Arato, E., 2023. Water absorption behavior and physico-chemical and mechanical performance of PLA-Based biopolymers filled with degradable glass fibers. J. Appl. Polym. Sci. 140 (43). https://doi.org/10.1002/app.54578.

Hussain, S., Akhter, R., Maktedar, S.S., 2024. Advancements in sustainable food packaging: from eco-friendly materials to innovative technologies. Sust. Food Technol 2, 1297–1364. https://doi.org/10.1039/D4FB00084F.

Iñiguez-Franco, F., Auras, R., Rubino, M., Dolan, K., Soto-Valdez, H., Selke, S., 2017. Effect of nanoparticles on the hydrolytic degradation of PLA-nanocomposites by water-ethanol solutions. Polym. Degrad. Stab. 146, 287–297. https://doi.org/10.1016/j.polymdegradstab.2017.11.004.

Khajavi, M.Z., Ebrahimi, A., Mortazavian, A.M., Farhoodi, M., Ahmadi, S., 2022. Hydrolytic degradation mechanism of modified polylactic acid in different food simulants. Food Packag. Shelf Life 34, 100956. https://doi.org/10.1016/j.fpsl.2022.100956.

Kong, Y., Hay, J.N., 2003. The enthalpy of fusion and degree of crystallinity of polymers as measured by DSC. Eur. Polym. J. 39, 1721–1727. https://doi.org/10.1016/S0014-3057(03)00054-5.

Lagazzo, A., Moliner, C., Finocchio, E., Caputo, S., Arato, E., 2025. Hydrolytic degradation and assessment of performance of PLA and PBS-based plastics designed for packaging applications. Int. J. Polym. Sci. 1–16. https://doi.org/10.1155/ijps/5602847.

Limsukon, W., Rubino, M., Rabnawaz, M., Lim, L.-T., Auras, R., 2023. Hydrolytic degradation of poly(lactic acid): unraveling correlations between temperature and the three phase structures. Polym. Degrad. Stab. 217, 110537. https://doi.org/10.1016/j.polymdegradstab.2023.110537.

Moeini, A., Pedram, P., Fattahi, E., Cerruti, P., Santagata, G., 2022. Edible polymers and secondary bioactive compounds for food packaging applications: antimicrobial, mechanical, and gas barrier properties. Polymers 14, 2395. https://doi.org/10.3390/polym14122395.

Moliner, C., Finocchio, E., Arato, E., Ramis, G., Lagazzo, A., 2020. Influence of the degradation medium on water uptake, morphology, and chemical structure of Poly (Lactic Acid)-Sisal Bio-composites. Materials 13, 3974. https://doi.org/10.3390/ma13183974.

Pedroni, M., Vasselolo, E., Aloiso, M., Brasca, M., Chen, H., Donnini, R., Firpo, G., Moarndi, S., Pietralunga, S.M., Silvetti, T., Speranza, G., Virgili, T., 2023. Nature-inspired antibacterial poly (butylene succinate) (PBS) by plasma etching nanotexturing for food packaging applications. Surf. Coating. Technol. 471, 129828. https://doi.org/10.1016/j.surfcoat.2023.129828.

Peng, G., Pu, Z., Chen, F., Xu, H., Cao, X., Chun Chen, C., Wang, J., Liao, Y., Zhu, X., Pan, K., 2023a. Metal leaching from plastics in the marine environment: an ignored role of biofilm. Environ. Int. 177, 107988. https://doi.org/10.1016/j.envint.2023.107988.

Peng, G., Pu, Z., Chen, F., Xu, H., Cao, X., Chun Chen, C., Wang, J., Liao, Y., Zhu, X., Pan, K., 2023b. Metal leaching from plastics in the marine environment: an ignored role of biofilm. Environ. Int. 177, 107988. https://doi.org/10.1016/j.envint.2023.107988.

Phua, Y.J., Chow, W.S., Mohd Ishak, Z.A., 2013. Reactive processing of maleic anhydride-grafted poly(butylene succinate) and the compatibilizing effect on poly (butylene succinate) nanocomposites. Express Polym. Lett. 7, 340–354. https://doi.org/10.3144/expresspolymlett.2013.31.

Phua, Y.J., Chow, W.S., Mohd Ishak, Z.A., 2011. The hydrolytic effect of moisture and hygrothermal aging on poly(butylene succinate)/organo-montmorillonite nanocomposites. Polym. Degrad. Stab. 96, 1194–1203. https://doi.org/10.1016/j.polymdegradstab.2011.04.017.

Platnieks, O., Gaidukovs, S., Kumar Thakur, V., Barkane, A., Beluns, S., 2021. Bio-based poly (butylene succinate): recent progress, challenges and future opportunities. Eur. Polym. J. 161, 110855. https://doi.org/10.1016/j.eurpolymj.2021.110855.

Rajgond, V., Mohite, A., More, N., More, A., 2024. Biodegradable polyester-polybutylene succinate (PBS): a review. Polym. Bull. 81, 5703–5752. https://doi.org/10.1007/s00289-023-04998-w.

Shen, K., 2023. Synthesis, properties and applications of poly (Butylene succinate). MATEC Web of Conferences 386, 01005. https://doi.org/10.1051/matecconf/202338601005.

Xu, D., Auras, R.A., Sonchaeng, U., Rubino, M., Lim, L., 2023. The effect of alcoholic solutions on the thermomechanical properties of immersed poly(lactic acid) films. J. Appl. Polym. Sci. 140. https://doi.org/10.1002/app.53489.

Yao, S.-F., Chen, X.-T., Ye, H.-M., 2017. Investigation of structure and crystallization behavior of Poly(butylene succinate) by fourier transform infrared spectroscopy. J. Phys. Chem. B 121, 9476–9485. https://doi.org/10.1021/acs.jpcb.7b07954.